Interaction of Nitric Oxide Synthase with the Postsynaptic Density Protein PSD-95 and α1-Syntrophin Mediated by PDZ Domains

Jay E. Brenman,* Daniel S. Chao,* Stephen H. Gee,‡
Aaron W. McGee,* Sarah E. Craven,*
Daniel R. Santillano,* Ziqiang Wu,* Fred Huang,*
Houhui Xia,† Matthew F. Peters,‡ Stanley C. Froehner,‡
and David S. Bredt*
*Department of Physiology
†Department of Pharmaceutical Chemistry
School of Medicine
University of California at San Francisco
San Francisco, California 94143
‡Department of Physiology
University of North Carolina at Chapel Hill
Chapel Hill, North Carolina 27599

Summary

Neuronal nitric oxide synthase (nNOS) is concentrated at synaptic junctions in brain and motor endplates in skeletal muscle. Here, we show that the N-terminus of nNOS, which contains a PDZ protein motif, interacts with similar motifs in postsynaptic density–95 protein (PSD-95) and a related novel protein, PSD-93. nNOS and PSD-95 are coexpressed in numerous neuronal populations, and a PSD-95/nNOS complex occurs in cerebellum. PDZ domain interactions also mediate binding of nNOS to skeletal muscle syntrophin, a dystrophin-associated protein. nNOS isoforms lacking a PDZ domain, identified in nNOS$^{\Delta/\Delta}$ mutant mice, do not associate with PSD-95 in brain or with skeletal muscle sarcolemma. Interaction of PDZ-containing domains therefore mediates synaptic association of nNOS and may play a more general role in formation of macromolecular signaling complexes.

Introduction

Endogenous nitric oxide (NO) derives from L-arginine as the product of a complex enzymatic reaction catalyzed by a family of three NO synthase (NOS) proteins (Moncada and Higgs, 1993; Bredt and Snyder, 1994a; Nathan and Xie, 1994). The neuronal isoform (nNOS or type I) is prominent in neurons and also occurs in epithelial cells of lung, in secretory cells of certain endocrine glands, and in skeletal muscle fibers (Schmidt et al., 1992; Kobzik et al., 1994). The endothelial NOS isoform (eNOS, type III) is abundant in all vascular endothelial cells and accounts for the endothelial-derived relaxing factor described by Zawadzki and Furchgott (1980). The inducible isoform (iNOS, type II) is rapidly upregulated in essentially all cell types following appropriate immunological stimuli and serves a nonspecific immune function (Hibbs et al., 1987).

Physiological studies have demonstrated numerous functions for neuron-derived NO. In the peripheral nervous system, NO functions as a nonadrenergic–noncholinergic neurotransmitter mediating actions of autonomic motor neurons on vascular and nonvascular smooth muscle. In brain, NO has been implicated in several forms of synaptic plasticity (for review, see Schuman and Madison, 1994). To help clarify functions for nNOS throughout the body, nNOS$^{\Delta/\Delta}$ mutant mice were generated with a targeted disruption of exon 2, which contains the predicted starter methionine codon (Huang et al., 1993). Initial analysis of nNOS mutant mice suggested a complete absence of nNOS protein and mRNA in brain and peripheral tissues. However, residual NOS catalytic activity was detected in brain at levels up to 8% of that found in wild-type animals (Huang et al., 1993). nNOS$^{\Delta/\Delta}$ mice suffer from hypertrophic pyloric stenosis (Huang et al., 1993), consistent with electrophysiological studies showing that NO mediates nonadrenergic–noncholinergic inhibitory junctional potentials at enteric sphincters. nNOS$^{\Delta/\Delta}$ mice are significantly resistant to brain injury following cerebral ischemia (Huang et al., 1994), consistent with a role for NO in this form of excitotoxicity (Dawson et al., 1992). nNOS mutant mice display an increase in aggressive behavior and excess and inappropriate sexual behavior (Nelson et al., 1995).

Synaptic actions of NO are facilitated by subcellular targeting of nNOS to specialized membrane structures. Biochemical studies indicate that nNOS partitions largely with membrane-associated and cytoskeletal subcellular fractions (Hecker et al., 1994; Brenman et al., 1995). Electron microscopy identifies >80% of nNOS immunoreactivity in monkey visual cortex as axonal or dendritic profiles (Aoki et al., 1993). Membrane-associated nNOS has also been identified at the sarcolemma of fast-twitch skeletal muscle fibers (Kobzik et al., 1994). Sarcolemmal targeting is mediated by association of nNOS with the dystrophin glycoprotein complex (Brenman et al., 1995). The absence of dystrophin in Duchenne muscular dystrophy results in translocation of nNOS from sarcolemma to muscle cytosol.

The N-terminal domain of nNOS is unique to the neuronal isoform and contains a PDZ/GLGF motif of ~100 amino acids that is found in a diverse group of cytoskeletal proteins and enzymes (Cho et al., 1992). Because this domain mediates association of nNOS with the dystrophin complex (Brenman et al., 1995), we have now used the yeast two-hybrid system to identify interacting proteins. Screening a brain library demonstrates that the PDZ-containing domain of nNOS binds to PDZ repeats in postsynaptic density 95 (PSD-95) (Cho et al., 1992) and a novel related protein, PSD-93. PSD-95 is coexpressed with nNOS in several neuronal populations in the developing and mature nervous system, and a specific PSD-95/nNOS interaction can be detected in transfected cell lines and solubilized cerebellar membranes. In skeletal muscle, we determine that association of nNOS with the sarcolemma is mediated by direct binding of nNOS to α1-syntrophin, a protein of the dystrophin complex containing a PDZ motif (Adams et al., 1993; Adams et al., 1995). Residual catalytically active nNOS isoforms we now identify in nNOS$^{\Delta/\Delta}$ mice, which specifically lack a PDZ motif, do not interact with PSD-95, nor do they associate with the dystrophin complex of skeletal muscle sarcolemma. These data demonstrate

Table 1. Interactions of nNOS and PSD-95/93 and α1-Syntrophin

Gal4 DNA Binding Hybrid	Gal4 Activation Hybrid	Colony Color	Growth
Interactions between nNOS and PSD-95 or PSD-93			
nNOS (amino acids 1–195)	SV 40 (amino acids 84–708)	White	−
p53 (72–390)	PSD–95, PDZ1–3 (20–364)	White	−
Lamin C (66–230)	PSD–95, PDZ1–3 (20–364)	White	−
nNOS (1–195)	PSD–95, PDZ1–3 (20–364)	Blue	+
nNOS (1–195)	PSD–95, PDZ1–2 (20–294)	Blue	+
nNOS (1–195)	PSD–95, PDZ2–3 (138–364)	Blue	+
nNOS (1–195)	PSD–95, PDZ1 (20–144)	White	−
nNOS (1–195)	PSD–95, PDZ2 (138–294)	Blue	+
nNOS (1–195)	PSD–95, PDZ3 (291–364)	White	−
p53 (72–390)	PSD–93 (116–421)	White	−
Lamin C (66–230)	PSD–93 (116–421)	White	−
nNOS (1–195)	PSD–93 (116–421)	Blue	+
p53 (72–390)	SV 40 (84–708)	Blue	+
Interaction between nNOS and α1-Syntrophin			
Lamin C (66–230)	α1-syntrophin (59–166)	White	−
p53 (72–390)	α1-syntrophin (59–166)	White	−
nNOS (1–195)	α1-syntrophin (59–166)	Lt. Blue	+

Yeast HF7c and Y187 cells were cotransformed with expression vectors encoding various GAL4 binding domain and GAL4 activation domain fusion proteins. Each transformation mixture was plated on two synthetic dextrose plates, one lacking tryptophan and leucine and the other lacking tryptophan, leucine, and histidine. Growth was measured on histidine-deficient plates, and color was measured by a β-galactosidase colorimetric filter assay (Fields and Song, 1989).

a physiological role for PDZ domain interactions in organizing proteins at synaptic membranes, and identify one potential function for PDZ domains in PSD-95 and α1-syntrophin.

Results

The PDZ-Containing Domain of nNOS Can Bind to Similar Motifs in PSD-95 and to a Related Protein, PSD-93

We fused the PDZ domain of nNOS (amino acids 1–195) to the DNA binding domain of GAL4 and screened a human brain library for interacting proteins using the yeast two-hybrid system (Fields and Song, 1989; Clonetech). Two families of interacting clones were identified from a screen of 10^6 plasmids (Table 1). One family represented isolates encoding the PDZ motifs of PSD-95, and the other family encoded PDZ repeats of a related novel gene product.

PSD-95 was originally identified as an abundant detergent insoluble component of brain postsynaptic density (Cho et al., 1992). Subcellular and electron micrographic studies have determined that PSD-95 occurs at both pre- and postsynaptic membrane specializations, similar to the distribution of nNOS (Aoki et al., 1993; Kistner et al., 1993). PSD-95 contains three PDZ repeats, an SH3 domain, and a region homologous to guanylate kinase (Cho et al., 1992). Our cloning and sequencing of the related gene predicts a protein of 93 kDa, PSD-93, that has the same domain structure as PSD-95 and shares 60% amino acid identity (the nucleotide sequence of PSD-93 has been deposited in GenBank).

nNOS and PSD-95 Are Colocalized in Adult and Developing Neurons

If the association of nNOS with PSD-95 identified in yeast is physiologically relevant, the two proteins must be coexpressed in neurons. In situ hybridization in rat brain (Figures 1a and 1b) demonstrated coexpression of nNOS and PSD-95 transcripts in several neuronal populations, particularly in cerebellar granule and basket cells, which have previously been shown to express high densities of nNOS and PSD-95 proteins (Bredt et al., 1990; Kistner et al., 1993). On the other hand, PSD-93 occurred at highest densities in cerebellar Purkinje neurons, complimentary to the distribution to nNOS and PSD-95.

We also compared expression of nNOS with PSD-95/93 during embryonic development. Using in situ hybridization, we found that nNOS-containing cells in embryonic day 15 (E15) rat were differentially coexpressed with either PSD-95 or PSD-93 (Figures 1c and 1d). As previously reported, transient nNOS neurons were detected in developing cerebral cortical plate, olfactory epithelium, and sensory ganglia (Bredt and Snyder, 1994b). In all of these neuronal groups, we found PSD-95 mRNA. nNOS was also developmentally expressed in certain nonneuronal cells including chromaffin cells of the adrenal gland and secretory cells of the submandibular gland. PSD-93 mRNA and nNOS mRNA were coexpressed in these glands, while PSD-95, which is reported to be neuron specific (Cho et al., 1992; Kistner et al., 1993), was absent.

Colocalization of nNOS and PSD-95 proteins was evaluated by immunohistochemical staining of adjacent sections from E19 rat. Within the olfactory system, both PSD-95 and nNOS were enriched in dendritic specializations in olfactory cilia and in axonal processes projecting to the olfactory bulb, which itself does not contain either nNOS or PSD-95 (Figures 2A–2D). nNOS also occurs in fetal myenteric neurons, and its absence is associated with hypertrophic pyloric stenosis. Immunohistochemical analysis revealed a colocalization of nNOS with PSD-95 in myenteric neurons (Figures 2E–2H). nNOS and PSD-95 were similarly colocalized in embryonic cerebral cortex. Staining for both proteins was enriched in the intermediate zone and developing cortical plate, while
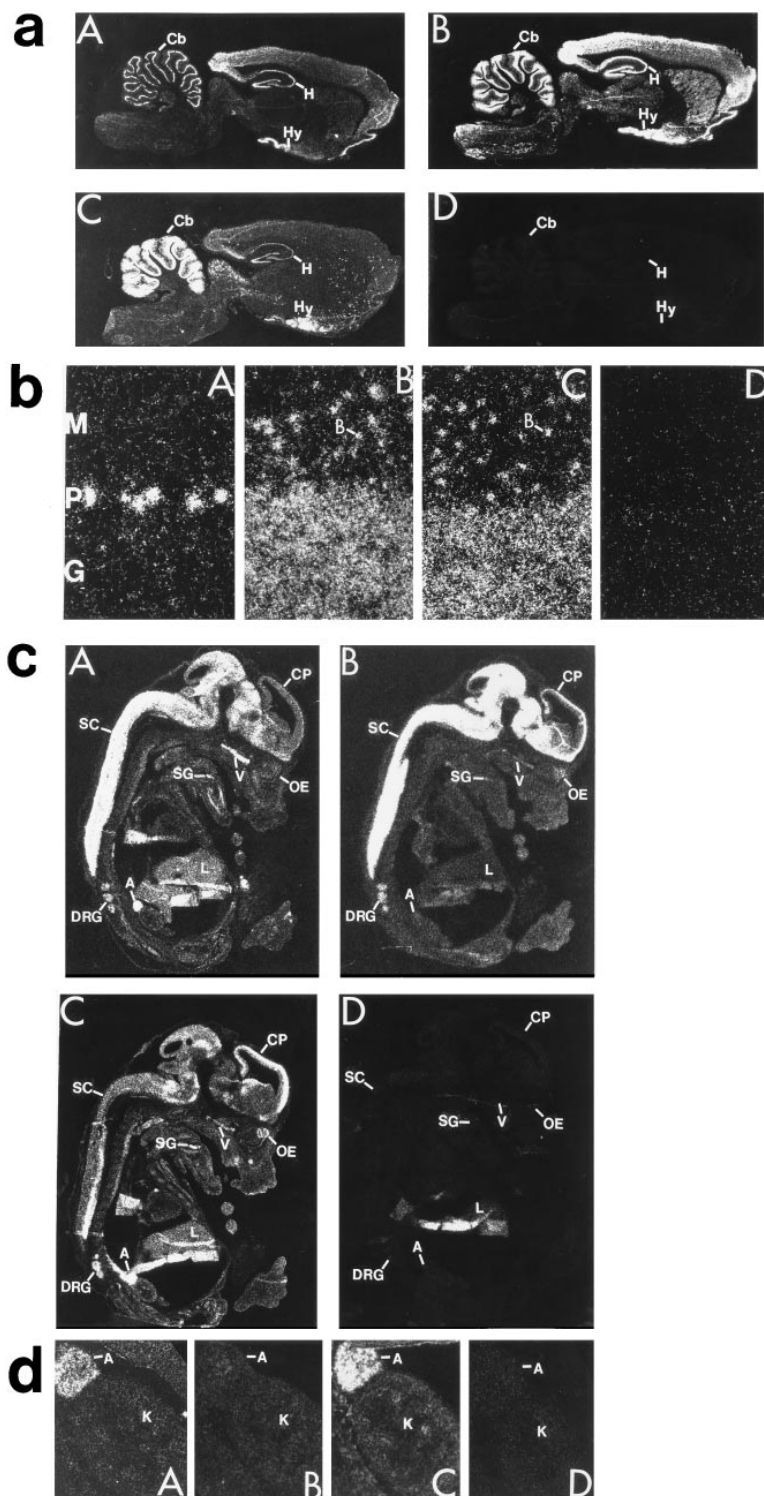
Figure 1. Expression of PSD-93, PSD-95, and nNOS in Rat Brain and E15 Embryo

In situ hybridization was used to localize transcripts for PSD-93 (A), PSD-95 (B), nNOS (C), or sense control (D) in adjacent cryosections. (a) In adult rat brain, PSD-95 occurred only in neurons and was coexpressed with nNOS in certain neurons in hypothalamus, hippocampus, and cerebellum. PSD-93 also appeared to be neuron specific but had a more restricted distribution than did PSD-95. (b) In cerebellum, PSD-95 and nNOS were coexpressed in cerebellar granule cells in the granular layer (G) and basket cells (B) in the molecular layer. By contrast, PSD-93 was restricted to Purkinje neurons (P) of cerebellum, which lack nNOS or PSD-95. Double labeling with reduced nicotinamide adenine dinucleotide phosphate diaphorase and in situ hybridization identified the PSD-95– and nNOS-expressing cells in molecular layer as basket cells (data not shown). (c) In E15 embryo, PSD-95 was found ubiquitously expressed in differentiated central neurons, but not in neuronal precursors. PSD-95 was coexpressed with nNOS in cerebral cortical plate (CP), dorsal root ganglia (DRG), and neurons of the olfactory epithelium (OE). PSD-93 was abundantly expressed in neurons of spinal cord (SC), DRG, and trigeminal nerve (V). PSD-93 was specifically coexpressed with nNOS in secretory cells of the submandibular gland (SG) and (d) in chromaffin cells of the developing adrenal gland, which lack PSD-95. The signal in liver (L) seen in all samples including control represents nonspecific hybridization to an aberrant fold in the tissue. K, kidney; A, adrenal gland.

lesser staining was found in the subplate region. The ventricular zone was devoid of staining (Figures 2I–2J).

nNOS Interacts with the Second
PDZ Motif of PSD-95
We found that an nNOS/PSD-95 complex was immunoprecipitated from COS cells cotransfected with expression vectors for nNOS and the PDZ repeats of PSD-95, indicating that this interaction occurs in a cellular environment (Figure 3A). To evaluate formation of an nNOS/PSD-95 complex in brain, we conducted immunoprecipitation studies. Though only a small fraction of PSD-95 can be solubilized from brain densities with nondenaturing detergents (Cho et al., 1992; Kistner et al., 1993), we specifically immunoprecipitated an nNOS/PSD-95 complex from cerebellum (Figures 3B and 3C), where both proteins are coexpressed at high levels.

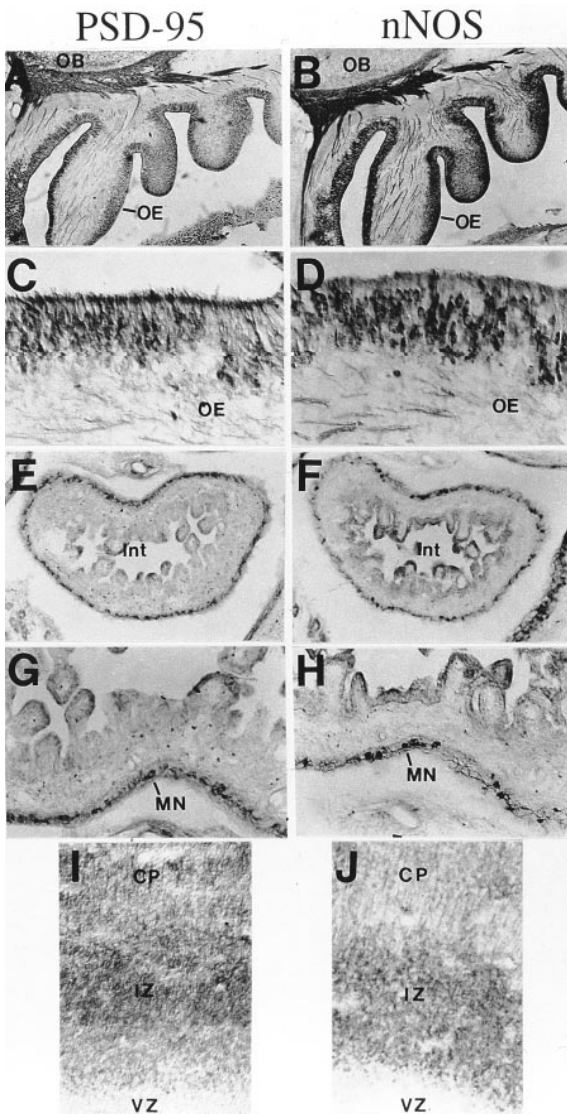Functions for PSD-95 are largely unknown. Recent

Figure 2. PSD-95 Colocalizes with nNOS in Developing Neurons

Immunohistochemical staining of adjacent sagittal sections of E19 rat fetus indicates that PSD-95 (A and C) and nNOS (B and D) are colocalized in primary olfactory epithelium (OE) and in nerve processes projecting to the olfactory bulb (OB) (A and B, 47×; C and D, 376×). In intestine (Int) of E19 rat, PSD-95 (E and G) and nNOS (F and H) are colocalized in myenteric neurons (MN) (E and F, 47×; G and H, 188×). In E19 rat cerebral cortex, PSD-95 (I) and nNOS (J) are again colocalized. Both proteins are most concentrated in neuronal processes of the intermediate zone (IZ) and cell bodies of the cortical plate (CP), while the ventricular zone (VZ) is devoid of staining (94×).
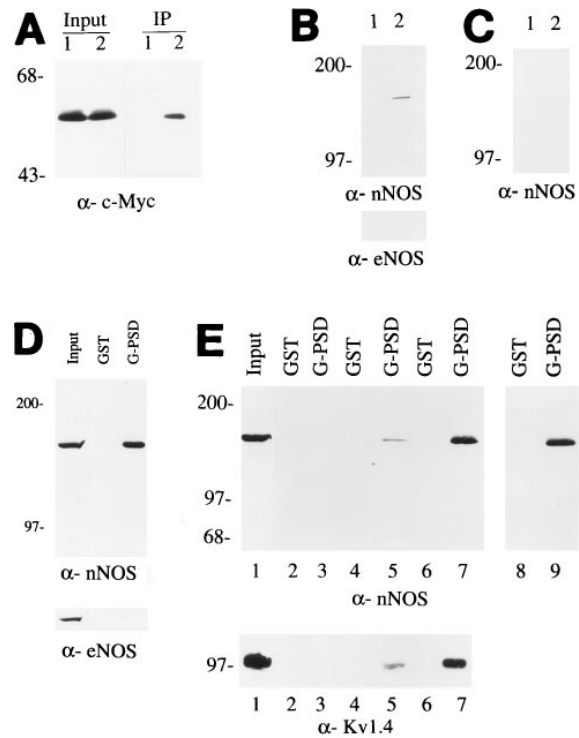

Figure 3. nNOS Binds to PSD-95 through PDZ Motif Interactions

(A–C) Coimmunoprecipitation of nNOS and PSD-95. (A) COS cells were transfected with an expression construct (PSD-myc) encoding amino acids 1–386 of PSD-95 with a 10 amino acid c-myc epitope tag alone (lanes 1) or were cotransfected with PSD-myc and nNOS (lanes 2). Cell homogenates were immunoprecipitated with nNOS and probed with a monoclonal antibody to c-myc. Input = 5% of protein loaded onto columns. (B) Solubilized cerebellar membranes were immunoprecipitated with antibody to PSD-95 (lanes 2) or a nonimmune serum (lanes 1). Western blotting shows specific coimmunoprecipitation of nNOS but not eNOS with PSD-95. (C) Identical immunoprecipitations from cerebellar cytosol, which lacks PSD-95 but contains high concentrations of nNOS, showed that the PSD-95 antibody (lane 2) does not directly interact with nNOS. The eNOS blot and the nNOS blot from cerebellar cytosol were intentionally overexposed, but failed to show specific immunoprecipitated bands. (D) Affinity chromatography demonstrates that nNOS is selectively retained by an immobilized PSD-95 protein fragment (amino acids 1–386) fused to GST. eNOS is not retained by the PSD column. Solubilized brain extracts were incubated with G-PSD or control GST beads, columns were washed with buffer containing 0.5 M NaCl and 1% Triton X-100, and eluted with SDS. Bound proteins were detected by Western blotting. Input = 10%. (E) NMDA receptor 2B carboxy-terminal peptide displaces nNOS and $K_v1.4$ from PSD-95. "Pull-down" assays from brain were conducted as above containing 0 (lanes 6 and 7), 10 μM (lanes 4 and 5), or 30 μM (lanes 2 and 3) NMDA receptor peptide or 200 μM control peptide (lanes 8 and 9). Input = 10%.

studies show that the second PDZ motif of PSD-95 interacts with certain ion channels in brain, including NMDA receptors and voltage-gated K^+ channels, that contain a carboxy-terminal tSXV consensus sequence (Kim et al., 1995; Kornau et al., 1995). To determine which domain(s) of PSD-95 bind to nNOS, we engineered yeast constructs encoding appropriate fragments of PSD-95 fused to the GAL4 activation domain. Constructs encoding the second PDZ motif of PSD-95 interacted with

nNOS, whereas those lacking this region were inactive (Table 1).

To biochemically evaluate these interactions, we generated a fusion protein linking glutathione S-transferase (GST) to the first 386 amino acids of PSD-95 (G-PSD). Solubilized brain extracts were incubated with glutathione beads linked to GST or G-PSD. Following extensive washing with buffer containing 350 mM NaCl and 0.5% Triton X-100, bound proteins were eluted with loading buffer. Western blotting indicated selective retention of

nNOS to G-PSD beads (Figure 3D). eNOS, which is 60% identical to nNOS but lacks a PDZ motif, was not retained by the G-PSD beads, indicating specificity of the interaction with nNOS.

Because the second PDZ motif of PSD-95 binds both to nNOS and to tSXV-containing ion channels, we determined whether these binding sites are independent or overlapping. Previous studies demonstrated that a peptide, corresponding to the carboxy-terminal 9 amino acids of NMDA receptor type 2B, blocks interaction of NMDA receptor with PSD-95 (Kornau et al., 1995). Similarly, we found that this NMDA receptor peptide potently blocks association of nNOS with PSD-95 (Figure 3E). Half-maximal inhibition of binding was achieved at <10 μM NMDA receptor peptide, whereas control peptides were inactive at 200 μM. As a control, we found that $K_v1.4$, a voltage-dependent K^+ channel containing a tSXV sequence, was displaced from PSD-95 by similar concentrations of NMDA receptor peptide. We also found that the second PDZ domain of PSD-93, expressed as a GST fusion protein, binds to nNOS in a manner competitive with the NMDA receptor peptide (data not shown).

Catalytically Active nNOS Isoforms Lacking a PDZ Motif Occur in nNOS$^{\Delta/\Delta}$ Mice

To further characterize the importance of the PDZ domain, we took advantage of our observation that mice carrying a targeted disruption of exon 2 of nNOS, express residual nNOS isoforms specifically lacking the PDZ domain. nNOS$^{\Delta/\Delta}$ mice were generated by deleting the first translated exon (Huang et al., 1993), which is exon 2 of nNOS in both mouse and human (Hall et al., 1994; see below) and which encodes the PDZ motif. Northern blotting and 5' rapid amplification of cDNA ends/polymerase chain reaction (RACE-PCR) analyses demonstrate that residual nNOS mRNAs are expressed in brain of nNOS$^{\Delta/\Delta}$ mice resulting from alternative splicing that skips the targeted 1.1 kb second exon (Figure 4). Interestingly, PCR and sequence analysis indicated that this alternative splice also occurs in wild-type mice and represents ~5% of total NOS mRNA (Figure 4C, lane 2).

Western blotting of purified brain extracts identified residual nNOS proteins of 136 and 125 kDa from nNOS$^{\Delta/\Delta}$ (Figure 5A, lanes 3 and 4). These 136 kDa (nNOSβ) and 125 kDa (nNOSγ) bands from nNOS$^{\Delta/\Delta}$ did not cross-react with antibodies to eNOS or iNOS (data not shown). Failure of previous studies to detect immunoreactive nNOS protein in nNOS$^{\Delta/\Delta}$ was due to the use of a less potent polyclonal antibody and a less sensitive colorimetric detection system (Huang et al., 1993).

To determine the relationship between the two transcripts identified by RACE-PCR and the two immunoreactive protein bands, COS cells were transfected with constructs corresponding to the truncated forms found in nNOS$^{\Delta/\Delta}$, that is, 5'a or 5'b spliced to exon 3. Transfection of the 5'a–containing construct generated a prominent immunoreactive protein band of 136 kDa that comigrated with nNOSβ from nNOS$^{\Delta/\Delta}$ brain (Figure 5B; lanes 3 and 4). Transfection of the 5'b–containing construct yielded an nNOS band of 125 kDa (Figure 5B, lane 5).

Catalytic assays indicated that the 136 kDa nNOSβ form had activity ~80% that of full-length nNOS under these transfection conditions (Figure 5C). Enzyme activity was fully dependent on calcium/calmodulin and the K_m for arginine was similar to that of full-length nNOS from brain. By contrast, the activity of the 125 kDa nNOSγ was ~3% that of nNOS.

NOS activity in wild-type brain is highest in cerebellum (Bredt et al., 1990). By contrast, NOS activity in nNOS$^{\Delta/\Delta}$ is highest in the striatum and lowest in the cerebellum (Huang et al., 1993). The regional distribution of residual nNOS isoforms in nNOS$^{\Delta/\Delta}$ brain extracts paralleled the pattern of residual nNOS activity previously reported (Figures 5D) (Huang et al., 1993).

nNOS Isoforms Lacking a PDZ Motif Do Not Associate with PSD-95 or Brain Membranes

nNOS$^{\Delta/\Delta}$ mice therefore express nNOS isoforms specifically lacking the PDZ motif and can be used as an important tool to determine the functions for this domain in vivo. We first evaluated association of residual nNOS isoforms with PSD-95. nNOS proteins purified from wild-type and nNOS$^{\Delta/\Delta}$ mouse forebrain were subjected to pull-down assays as described above. Only full-length nNOS protein containing the PDZ motif was retained by G-PSD beads; the alternatively spliced forms in nNOS$^{\Delta/\Delta}$ did not adhere to G-PSD (Figure 6A). We also compared the distribution of nNOS in wild-type and nNOS$^{\Delta/\Delta}$ mouse by subcellular fractionation. Brain homogenates were first extracted with physiological saline, then with buffer containing 1 M KCl and 1% Triton X-100, leaving a cytoskeletal pellet. nNOS in wild-type brain was present in all fractions, whereas residual nNOS isoforms in nNOS$^{\Delta/\Delta}$ occurred only in the first soluble fraction (Figure 6B).

nNOS Binds to Skeletal Muscle Syntrophin through PDZ Interactions

Interaction of PDZ motifs in nNOS and PSD-95 raised the possibility that the PDZ domain of syntrophin (Adams et al., 1995) represents the binding site for association of nNOS with the dystrophin complex (Brenman et al., 1995). Interaction between the PDZ-containing domains of nNOS (amino acids 1–195) and α1-syntrophin (amino acids 59–166) was first evaluated by the yeast two-hybrid system. When cotransfected, these constructs reconstituted GAL4 transcriptional activity (Table 1).

To biochemically evaluate association, we first conducted "pull-down" assays from skeletal muscle extracts using GST fused to the PDZ domain of nNOS (G-NOS; Brenman et al., 1995). α1-syntrophin was selectively retained by this column but did not associate with a control GST protein column (Figure 7A; lanes 1, 3, and 4). We previously demonstrated that dystrophin is retained by a G-NOS column (Brenman et al., 1995). The absence of dystrophin in mdx mouse results in disruption of the dystrophin glycoprotein complex. We therefore evaluated association of skeletal muscle syntrophin from mdx mouse with G-NOS. Total α1-syntrophin levels were decreased ~50% in mdx muscle, in agreement with previous findings (Butler et al., 1992). Binding of α1-syntrophin to G-NOS was unaffected by dystrophin deficiency (Figure 7A; lanes 2, 5, and 6). To demon-
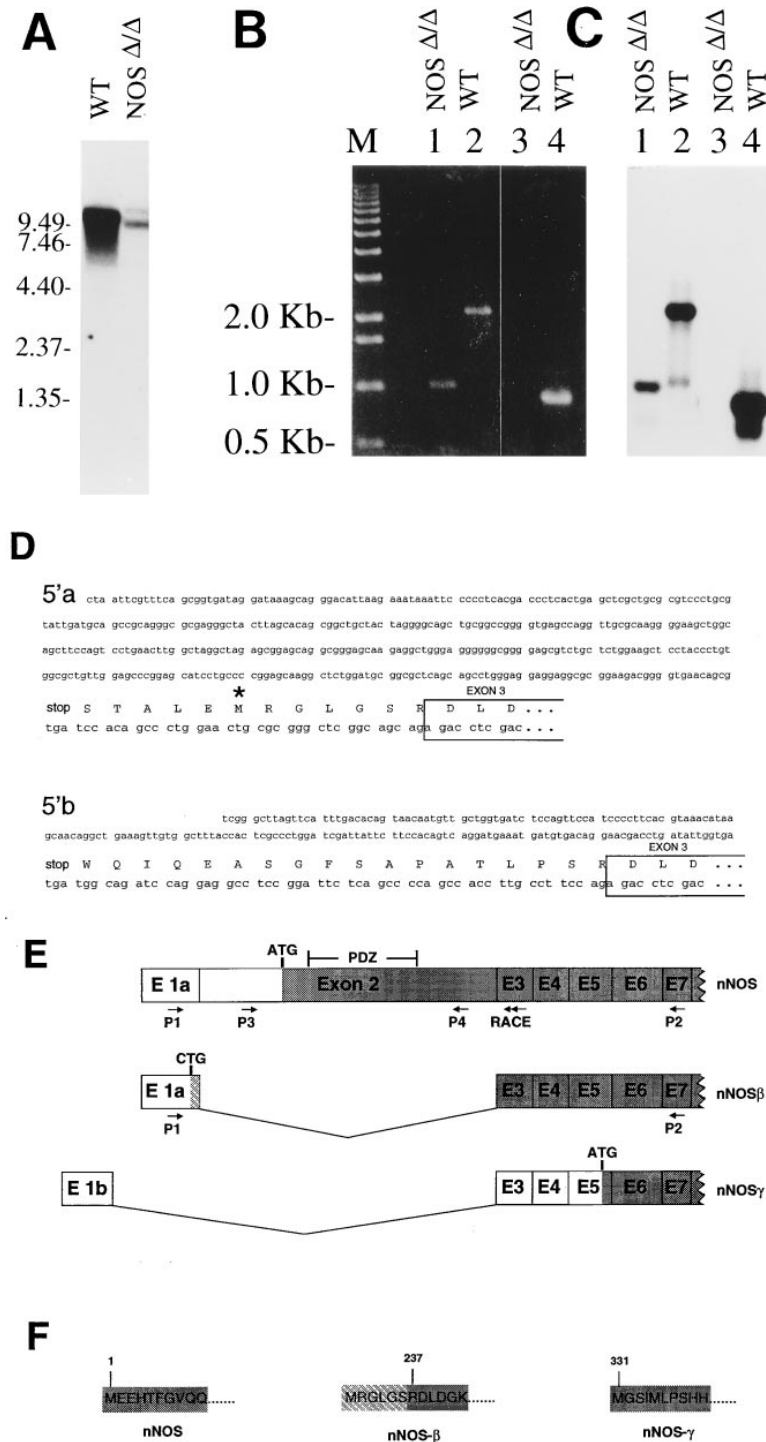
A

9.49-
7.46-
4.40-
2.37-
1.35-

WT   NOS Δ/Δ

B

M   1   2   3   4

2.0 Kb-
1.0 Kb-
0.5 Kb-

NOS Δ/Δ   WT   NOS Δ/Δ   WT

C

1   2   3   4

NOS Δ/Δ   WT   NOS Δ/Δ   WT

D

5'a cta attcgtttca gcggtgatag gataaagcag ggacattaag aaataaattc cccctcacga ccctcactga gctcgctgcg cgtccctgcg

tattgatgca gccgcagggc gcgagggcta cttagcacag cggctgctac taggggcagc tgcggccggg gtgagccagg ttgcgcaagg ggaagctggc

agcttccagt cctgaacttg gctaggctag agcggagcag gcgggagcaa gaggctggga gggggcggg gagcgtctgc tctggaagct cctaccctgt

ggcgctgttg gagcccggag catcctgccc cggagcaagg ctctggatgc ggcgctcagc agctcgggag gaggaggcgc ggaagacgggg gtgaacagcg

stop S   T   A   L   E   M* R   G   L   G   S   R | D   L   D . . .
     tga tcc aca gcc ctg gaa ctg cgc ggg ctc ggc agc aga | gac ctc gac . . .

                                                           EXON 3

5'b   tcgg gcttagttca tttgacacag taacaatgtt gctggtgatc tccagttcca ttcccttcac gtaaacataa

gcaacaggct gaaagttgtg gctttaccac tcgccctgga tcgattattc ttccacagtc aggatgaaat gatgtgacag gaacgacctg atattggtga

stop W   Q   I   Q   E   A   S   G   F   S   A   P   A   T   L   P   S   R | D   L   D . . .
     tga tgg cag atc cag gag gcc tcc gga ttc tca gcc cca gcc acc ttg cct tcc aga | gac ctc gac . . .

                                                                                EXON 3

E

F

Figure 4. Exons 1 and 2 of nNOS Are Alternatively Spliced

(A) Northern blot analysis of brain mRNA from wild-type (WT) and nNOS$^{\Delta/\Delta}$ mouse hybridized with a full-length nNOS cDNA probe. A broad band of 10.5 kb is recognized in wild-type brain and weaker bands of 11 and 9.5 kb are recognized in nNOS$^{\Delta/\Delta}$ mouse. (B and C) RT-PCR analysis of 5′ splicing of nNOS gene. cDNA was amplified with primers 1 and 2 (lanes 1 and 2). (B) Ethidium bromide staining shows a band of 1 kb amplified from nNOS$^{\Delta/\Delta}$ and a band of 2.2 kb from wild type. (C) Southern hybridization with a full-length nNOS probe shows hybridization to the ethidium-stained bands. A weaker band of 1 kb in amplifications of wild-type cDNA is also detected by hybridization (C, lane 2). A similar analysis using primers 3 and 4 confirm that exon 2 sequences are only detected in wild-type cDNA (lanes 3 and 4). (D) Nucleotide sequences of 5′ RACE-PCR products amplified from nNOS$^{\Delta/\Delta}$ brain. Predicted CTG starter methionine in 5′a is marked with an asterisk. (E) Schematic diagram of exon structure of nNOS isoforms (exon structure beyond 2 is extrapolated from the human gene [Hall et al., 1994]). The predominant transcript in wild-type mice is shown on top. The two transcripts detected in nNOS$^{\Delta/\Delta}$ mice lacking exon 2 are shown below. Positions of PCR primers, intron/exon borders, and methionine start codons are noted. Translated sequences within nNOS are shaded. Unique N-terminal region of nNOSβ is cross-hatched. (F) Predicted N-terminal amino acid sequence of nNOS isoforms. Numbers correspond to amino acid positions within mouse nNOS.

strate association of nNOS with syntrophin in muscle extracts, we conducted immunoprecipitation experiments. A polyclonal antibody specific for α1-syntrophin selectively precipitated nNOS from solubilized skeletal muscle microsomes (Figure 7B). No precipitation of nNOS occurred with nonimmune antibody, and eNOS, was not specifically precipitated by the α1-syntrophin antibody (Figure 7C).

To determine the role of the PDZ domain for association of nNOS with sarcolemmal dystrophin complexes in

vivo, we evaluated the subcellular distribution of nNOS isoforms in nNOS$^{\Delta/\Delta}$ mouse. Skeletal muscle homogenates were sequentially extracted with physiologic saline, then 500 mM NaCl, and finally 0.5% Triton X-100. Following 2′5′ ADP agarose purification of these muscle extracts, Western blotting indicated that only the nNOSγ form is expressed in muscle of nNOS$^{\Delta/\Delta}$. This may be due to expression of unique alternative 5′ untranslated exons in skeletal muscle (Xie et al., 1995). nNOS in skeletal muscle runs as a doublet due to a 102 bp (34 amino
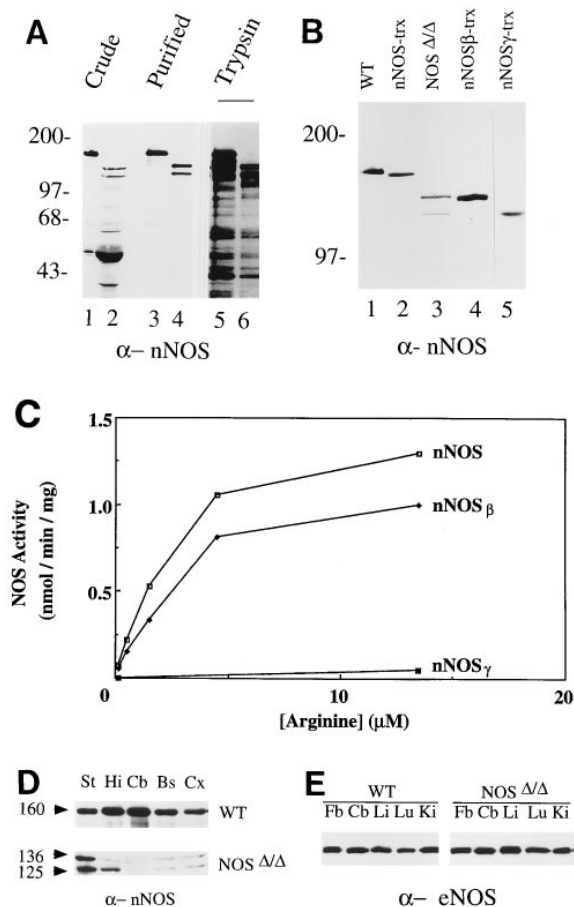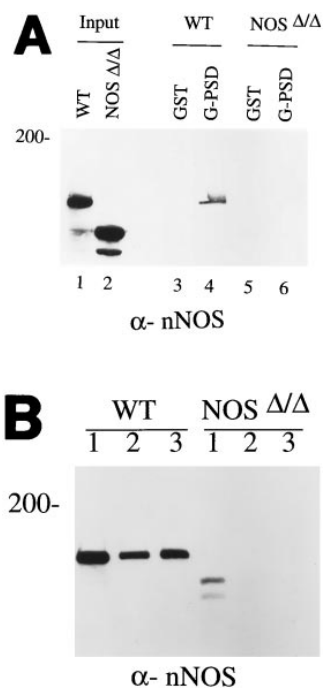
Figure 6. nNOS Isoforms Lacking the PDZ Motif Do Not Bind to PSD-95 or to Brain Membranes

(A) Partially purified nNOS protein from wild-type (WT) or nNOS$^{\Delta/\Delta}$ brain were analyzed by PSD "pull-down" assay. Full-length nNOS binds to PSD-95 while the residual isoforms lacking the PDZ motif do not. Input = 20%. (B) Residual nNOS isoforms are restricted to cytosol of nNOS$^{\Delta/\Delta}$. Brain homogenates, extracted with 100 mM NaCl (lanes 1), 1 M KCl + 1% Triton X-100 (lanes 2) or insoluble pellet (lanes 3), from wild-type (20 μg/lane) or nNOS$^{\Delta/\Delta}$ (200 μg/lane) were probed by Western blotting.

Figure 5. Catalytically Active nNOS Isoforms Lacking Exon 2 Are Expressed in Brain of nNOS$^{\Delta/\Delta}$

(A) Western blotting of crude (lanes 1 and 2) and 2'5'-ADP affinity-purified (lanes 3 and 4) brain extracts indicates that the major nNOS band in wild-type brain migrates at 160 kDa (lanes 1 and 3), whereas in nNOS$^{\Delta/\Delta}$, copurifying bands of 125 and 136 kDa (lanes 2 and 4) are recognized. Partial tryptic digestion of 2'5'-ADP agarose-purified proteins reveals a similar proteolytic "fingerprint" from wild type (lane 5) and nNOS$^{\Delta/\Delta}$ (lane 6). Note that 20-fold more protein was loaded from nNOS$^{\Delta/\Delta}$ (lanes 2, 4, and 6) than from wild-type samples (lanes 1, 3, and 5). (B) cDNA clones encoding nNOS, nNOSβ (5'a spliced to exon 3), or nNOSγ (5'b spliced to exon 3) were transfected (trx) into COS cells, and protein extracts were resolved by SDS–PAGE. Full-length NOS (nNOS-trx) comigrates at 160 kDa with the major product from wild-type brain (lanes 1 and 2). Transfection of nNOSβ and nNOSγ yields proteins of 136 and 125 kDa, respectively, that comigrate with immunoreactive bands from nNOS$^{\Delta/\Delta}$ (lanes 3–5). (C) NOS catalytic activity of nNOS isoforms. COS cells were transfected with 10 μg of expression vector encoding full-length nNOS, nNOSβ, or nNOSγ. NOS activity was measured in cell homogenates three days following transfection in the presence of 200 μM free calcium. This experiment was replicated twice with similar results. (D) nNOS isoforms are discretely expressed in nNOS$^{\Delta/\Delta}$ brain. Highest densities of nNOS in wild type (10 μg/lane) are found in cerebellum (Cb). In nNOS$^{\Delta/\Delta}$ (100 μg/lane) highest levels of nNOS isoforms are found in striatum (St) and hippocampus (Hi), lower amounts are found in brainstem (Bs) and cerebral cortex (Cx) while the cerebellum is devoid of nNOS isoforms in nNOS$^{\Delta/\Delta}$. (E) eNOS is homogeneously distributed in forebrain (Fb), cerebellum (Cb), as well as the peripheral tissues liver (Li), lung (Lu), and kidney (Ki). All lanes in (C) were loaded with 100 μg of solubilized membrane extract.

acid) alternative splice near the middle of the gene (H. Xia et al., unpublished data). Importantly, subcellular fractionation indicated that nNOSγ was restricted to soluble fractions of skeletal muscle (Figure 7E), contrasting with the soluble/particulate distribution of full-length nNOS in muscle (Figure 7D).

Protein overlay assays were performed to evaluate association of nNOS with individual domains of α1-syntrophin. The three known syntrophins (α1, β1, and β2) have a common domain structure consisting of two Pleckstrin homology (PH) domains, a PDZ domain and a carboxy-terminal domain unique to syntrophins (SU, syntrophin unique). Figure 8A shows the interaction between the nNOS–GST (1–299) fusion protein and the four α1-syntrophin domain fusion proteins, PH1, PDZ, PH2, and SU. Notably, only PDZ associates with nNOS. Moreover, no prominent bands were detected when the domains were overlayed with GST alone. Syntrophin domain fusion proteins (containing the T7·Tag epitope) were also used to overlay GST and nNOS–GST (Figure 8B). Again, only the PDZ domain of α1-syntrophin bound to nNOS, and no binding was observed to GST alone.

Discussion

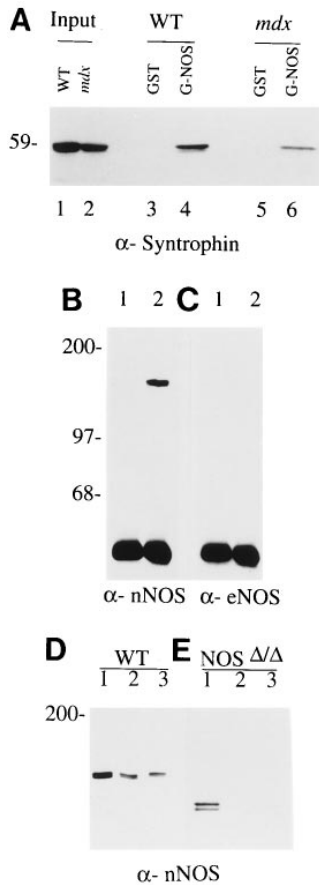The PDZ consensus sequence is present in a diverse family of enzymes and structural proteins. Many of these

Figure 7. α1-Syntrophin Binds to the N-terminal PDZ Containing Domain of nNOS

(A) "Pull-down" assays of solubilized muscle extracts from wild-type or *mdx* mouse using an nNOS (amino acids 1–299)-GST fusion protein were done as described in Figure 5. Western blotting shows that α1-syntrophin from both wild-type and *mdx* mouse is selectively retained by the G-NOS column. Input = 20%. (B and C) Immunoprecipitation of solubilized muscle extracts with a polyclonal antibody to α1-syntrophin shows coprecipitation of (B) nNOS but not (C) eNOS (lanes 2). Control experiments with nonimmune serum show no precipitation of nNOS or eNOS (lanes 1). Bands at 55 kDa represent immunoglobulin heavy chains. (D and E) Subcellular fractionation of nNOS is altered nNOS$^{\Delta/\Delta}$ mouse muscle. Homogenized muscle was sequentially extracted in buffer containing 100 mM NaCl (lanes 1), 500 mM NaCl (lanes 2), and 500 mM NaCl + 1% Triton X-100 (lanes 3). These extracts were purified by 2′5′-ADP agarose chromatography and were resolved by SDS–PAGE. (D) nNOS is present in both soluble and membrane-associated fractions of wild-type mouse, whereas (E) nNOS isoforms in nNOS$^{\Delta/\Delta}$ are restricted to the cytosol.

Figure 8. Direct Binding of nNOS to α1-Syntrophin PDZ Domain

(A) Purified α1-syntrophin PH1 (25 kDa; lanes 1), PDZ domain (15 kDa; lanes 2), PH2 (18 kDa; lanes 3), and SU domain (16 kDa; lanes 4) fusion proteins were resolved and overlayed with GST or nNOS (1–299)-GST. The position and relative amounts of the α1-syntrophin domain fusion proteins are indicated by immunoreactivity with a monoclonal against the T7·Tag. Bound GST fusion proteins were detected by blotting with a monoclonal antibody to GST. Only nNOS-GST bound specifically to the PDZ domain of α1-syntrophin. (B) GST (lanes 1) and nNOS-GST (lanes 2) were separated and overlayed with α1-syntrophin domain fusion proteins (PH1, PDZ, or PH2) or blotted with a monoclonal antibody to GST. Bound syntrophin fusion proteins were detected with monoclonal antibody to T7·Tag. Of the syntrophin fusion proteins tested, only PDZ bound to nNOS; no binding to GST was detected. (C) Colocalization of nNOS and α1-syntrophin immunofluorescence at skeletal muscle sarcolemma and neuromuscular junctions (labeled by rhodamine α-bungarotoxin). (D) Schematic model showing interaction of nNOS with skeletal muscle α1-syntrophin (59K syn). The possibility that other enzymes containing a PDZ motif may also bind to syntrophins is indicted at the left with question marks. DG, dystroglycan.

proteins are found concentrated at specialized cell–cell junctions, such as neuronal synapses, epithelial zona occludens, and septate junctions. These observations have motivated suggestions that PDZ domains may participate in protein–protein interactions at the plasma membrane (Cho et al., 1992). Our results support this idea and suggest that PDZ domains may be important elements in interactions required for signal transduction at the membrane.

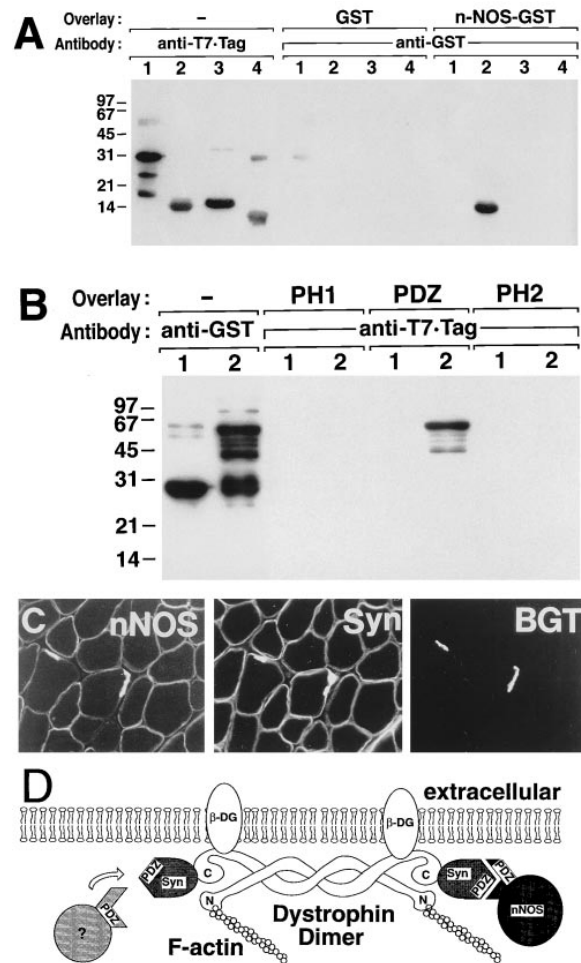The demonstration that nNOS directly interacts with the PDZ domain of α1-syntrophin explains the observed association of nNOS with sarcolemmal dystrophin complexes (Brenman et al., 1995). We also find that nNOS and α1-syntrophin share a similar distribution in skeletal muscle fast fibers (Figure 8C). The association of nNOS and α1-syntrophin may also account for the absence of nNOS from skeletal muscle sarcolemma in Duchenne

muscular dystrophy (Brenman et al., 1995). The three known isoforms of syntrophin (Adams et al., 1993; Ahn et al., 1994; Yang et al., 1994) each have a defined domain structure (Adams et al., 1995). The first PH domain, which begins near the N-terminus, is split by an insert that contains the PDZ domain. A second PH domain is followed by a highly conserved C-terminal domain with apparently no homology to known proteins. Although the binding site for dystrophin has not been definitively identified, recombinant fragments of β1-syntrophin beginning just downstream of the PDZ domains bind dystrophin and other members of the dystrophin protein family (Ahn and Kunkel, 1995). Since the syntrophins have highly conserved domain structures, the location of the dystrophin binding site is likely to be the same in all three syntrophins. Thus, the binding sites for nNOS and dystrophin appear to lie in distinct regions of α1-syntrophin. Together, these studies define syntrophin as a modular adapter protein linking a signaling enzyme, nNOS, to the sarcolemmal dystrophin complex. A model depicting these interactions is shown in Figure 8D.

Other proteins containing PDZ domains are likely to be recruited to the dystrophin complex through association with syntrophins. It will be of particular interest to identify proteins that bind to the PDZ domains of β1- and β2-syntrophin. Since the latter is highly localized to the neuromuscular postsynaptic membrane, it seems likely that proteins specifically associated with the PDZ domain of β2-syntrophin will be important in synaptic signaling. nNOS is enriched in fast-twitch muscle fibers in rat while α1-syntrophin is found in both fast and slow fibers. Therefore, depending on the muscle type, only a small fraction of α1-syntrophin may be associated with nNOS, thus allowing for interactions with other PDZ-containing proteins.

In brain, membrane association of nNOS does not require dystrophin (Brenman et al., 1995). Instead, we find that nNOS binds to the second PDZ repeat of PSD-95, and a related protein PSD-93. nNOS and PSD-95 are coexpressed in numerous populations of developing and mature neurons, and a PSD-95/nNOS complex can be identified in solubilized cerebellar membranes. Further evidence that the nNOS/PSD-95 interaction is physiological derives from electron micrographic studies showing that 83% of nNOS immunoreactive profiles in cerebral cortex occur in pre- and postsynaptic specializations of axon terminals and over thick postsynaptic densities (Aoki et al., 1993), similar to the distribution of PSD-95 (Cho et al., 1992; Kistner et al., 1993). nNOS also occurs in certain nonneuronal cells, including developing chromaffin cells of the adrenal gland and secretory cells of salivary gland. In these cells, nNOS is coexpressed with PSD-93, but not PSD-95. Definitive evidence that nNOS physiologically associates with PSD-93 in these glands will require development of antisera for coimmunoprecipitation studies in vivo.

The importance of the PDZ domain of nNOS is further revealed by our studies of nNOS$^{\Delta/\Delta}$ mouse. This work indicates that the residual NOS activity in brain of these mutants results from alternative splicing that skips the targeted second exon of nNOS. This alternative splicing also occurs at low levels in wild-type mice and results in truncated nNOS proteins lacking the PDZ motif encoded in exon 2. nNOS isoforms lacking the PDZ domain have altered subcellular distribution. We find that these isoforms do not adhere to PSD-95 from brain synaptic densities, nor do they associate with the dystrophin complex in skeletal muscle. This demonstrates a primary role for the PDZ domain in mediating subcellular localization of nNOS. Pyloric stenosis in nNOS$^{\Delta/\Delta}$ mice (Huang et al., 1993) may therefore be due to dyslocalization of nNOS, as we find that residual nNOS occurs at 5%–10% of normal levels in myenteric neurons of the mutant mice (J. E. Brenman et al., unpublished data). Behavior abnormalities of nNOS$^{\Delta/\Delta}$ mice (Nelson et al., 1995) may also be due to misexpression rather than lack of nNOS.

Binding interactions between PDZ domains are selective. Though nNOS binds to the PDZ motif in α1-syntrophin and to the second PDZ motif of PSD-95, nNOS does not associate with the first or third PDZ motifs in PSD-95. Certain PDZ domains are capable of binding to the extreme C-terminus of a family of receptors and ion channels, including NMDA receptors (Kim et al., 1995), Shaker-type K$^+$ channels (Kornau et al., 1995), and Fas, a receptor involved in the induction of apoptosis (Sato et al., 1995). These studies identify a C-terminal consensus tSXV that interacts with the second PDZ motif in PSD-95 and with the third PDZ motif of a protein tyrosine phosphatase, FAP-1, but not with the PDZ motif of nNOS (Kornau et al., 1995).

We find that the PDZ domain of nNOS and the tSXV motif of NMDA receptors compete for common or nearby binding sites within the second PDZ repeat of a PSD-95 subunit. However, PSD-95 can mediate K$^+$ channel clustering and likely occurs as an oligomeric complex (Kim et al., 1995). The binding of nNOS and NMDA receptors to distinct PSD-95 subunits in such a complex may contribute to the well-described functional coupling of NMDA receptors to NOS activity in cerebellum and forebrain (Garthwaite, 1991). Membrane permeant compounds that block association of nNOS with PSD-95 might therefore serve as novel therapeutics, as neuron-derived NO, associated with NMDA receptor activity, mediates brain injury following cerebral ischemia (Huang et al., 1994).

Experimental Procedures

Antibodies and Western Blotting

The following primary antibodies were used: nNOS1 polyclonal raised against homogenous nNOS protein purified from rat cerebellum (Bredt et al., 1990), nNOS monoclonal (Transduction Labs), eNOS monoclonal (Transduction Labs), iNOS monoclonal (Transduction Labs), α1-syntrophin polyclonal (Peters et al., 1994), PSD-95 polyclonal (Cho et al., 1992), K$_v$1.4 polyclonal (Kim et al., 1995), c-myc monoclonal (9E10; BABCO), T7·Tag monoclonal and GST 12 monoclonal (Santa Cruz Biotechnology). For Western blotting, protein extracts were resolved by SDS-polyacrylamide gel electrophoresis and transferred to PVDF membranes. Primary antibodies were diluted in block solution containing 3% bovine serum albumin, 0.1% Tween 20 in Tris-buffered saline and incubated with membranes overnight at 4°C. Labeled bands were visualized using enhanced chemiluminescence (Amersham). All nNOS Western blots used nNOS monoclonal.

In Situ Hybridization

In situ hybridization used ^{35}S-labeled RNA probes exactly as described (Sassoon and Rosenthal, 1993). Antisense probes to nNOS (nucleotides 4119–5057), PSD-95 (1–1155), PSD-93 (237–927) or

sense control PSD-93 (237–927) were synthesized from Bluescript vectors.

Immunohistochemistry

Rats were perfused with 4% paraformaldehyde, tissues were harvested, postfixed at 4°C for 3 hr, and cryoprotected in 20% sucrose overnight. Sections (20 μm) were cut on a cryostat and melted onto glass slides (Plus, Fisher). Sections were then blocked for 1 hr in buffer containing 2% goat serum, 0.1% Triton X-100 in phosphate-buffered saline. Primary antibodies to nNOS (polyclonal nNOS), PSD-95, or α1-syntrophin were diluted into blocking reagent and incubated with sections overnight. Immunoperoxidase histochemistry was performed using the ABC method (Vector). Immunofluorescent staining of rat extensor digitorum longus muscle was done as described (Brenman et al., 1995). Control sections lacking primary antisera were stained in parallel.

Cell Culture and Transfection

Neuronal NOS cDNAs were cloned into the EcoRV and XbaI sites of the mammalian expression vector pcDNA 3 (Invitrogen). 5′a– and 5′b–containing constructs were amplified by PCR, sequenced, and cloned into the unique NarI restriction site of nNOS. PSD-95-myc construct (amino acids 1–386 with a C-terminal myc-epitope tag) was amplified by PCR and cloned into the BamHI and EcoRI sites of pcDNAIII. Monkey COS cells were grown and transfected using calcium phosphate as previously described (Bredt et al., 1991). Two days following transfection, cells were washed with phosphate-buffered saline, harvested in 2 ml of buffer containing 25 mM Tris–HCl (pH 7.4), 100 mM NaCl, 1 mM EDTA, 1 mM EGTA, 1 mM phenylmethylsulfonyl fluoride and disrupted using a polytron.

Immunoprecipitations

Rat cerebellum was homogenized in 20 vol of buffer containing 25 mM Tris (pH 7.5), 150 mM NaCl and centrifuged at 100,000× g to yield cytosol. Cerebellar membranes were solubilized with 1% digitonin and 100 mM NaCl and centrifuged to remove the insoluble cytoskeleton. PSD-95 polyclonal antiserum to PSD-95 (3 μl) or nonimmune serum (3 μl) was added to 1 ml (500 μg) of cerebellar cytosol or solubilized membranes. After a 60 min incubation on ice, 50 μl of protein A sepharose was added to precipitate antibodies. Protein A pellets were washed 3 times with buffer containing 200 mM NaCl and 1% Triton X-100. Immunoprecipitated proteins were denatured with loading buffer and resolved by SDS-PAGE. Heavy microsomes of rat gastrocnemius were prepared and solubilized with 1% Triton X-100 as described (Brenman et al., 1995). Polyclonal antiserum to α1-syntrophin (5 μg) or nonimmune serum (5 μg) was added to 1 ml (500 μg) solubilized muscle samples. Immunoprecipitations from transfected COS cells used polyclonal antibody to nNOS.

GST Fusion Protein Affinity Chromatography

GST fusion constructs were constructed by PCR and fusion proteins purified as previously described (Brenman et al., 1995). For "pull down" assays, solubilized tissue samples were incubated with control or GST-fusion protein beads for 1 hr. Beads were washed with buffer containing 0.5% Triton X-100 + 350 mM NaCl, and proteins eluted SDS loading buffer. NMDA receptor peptide (KLSSIESDV) or control peptide (KPKHAKHPDGHSGNLC) were added where indicated during tissue incubation with the fusion protein.

Generation of α1-Syntrophin Fusion Proteins and Protein Overlay Assay

cDNAs encoding mouse α1-syntrophin domains (PH1a domain, amino acids 1–77; PH1b, 162–271; PDZ, 75–170; PH2, 281–402; SU domain 401–499) were amplified by PCR and cloned into pET28a vector (Novagen), with the exceptions of PH1a and PH1b, which were ligated together to produce the intact PH1 domain. Clones were sequenced and electroporated into BL21(λDE3)pLysS cells. Overnight cultures were diluted 1:10, incubated 2 hr, and induced for 3 hr with isopropyl-β-D-thiogalactopyranoside; and expressed proteins, which contain a T7·Tag epitope encoded in the vector, were purified on Nickel columns (Novagen). The PH1 and PDZ domains were purified from the soluble fraction; PH2 and SU were purified from urea-solubilized inclusions. Fusion proteins were separated on 15% SDS–PAGE gels, transferred to nitrocellulose membranes, blocked with 5% skim milk in 25 mM Tris (pH 7.5), 150 mM NaCl, and 0.1% Tween-20 (Tris-buffered saline/Tween) and incubated with purified fusion proteins (20 μg/ml) in this buffer for 1 hr at 25°C. Blots were washed 3× 10 min in Tris-buffered saline/Tween, incubated with primary antibody T7·Tag or GST 12 for 30 min and bands visualized by enhanced chemiluminescence.

mRNA Isolation and cDNA Analysis

RNA was isolated using the guanidine isothiocyanate/CsCl method, and mRNA was selected using oligo dT sepharose. For Northern blotting, mRNA was separated on a formaldehyde agarose gel and transferred to a Nylon membrane. A random-primed ^{32}P probe was generated using the full-length (5057 bp) nNOS cDNA (Bredt et al., 1991) as a template. The filter was washed at high stringency, 68°C, 0.1% sodium chloride/sodium citrate, 0.1% SDS and exposed to X-ray film overnight at −70°C.

Thermal RACE-PCR was performed as described (Frohman, 1993). The sequences of the nNOS-specific primers in exon 3 were as follows: Race 1, CCACAGATCATTGAAGACTCG; Race 2, GGGGA ATTCCCCGCCCAGGGGCGGAGCTTT.

For RT–PCR, mRNA was reverse transcribed with RTth polymerase using random hexamer primers. The sequences of the PCR primers used were as follows: P1, GTCCCTGCGTATTGATGCA; P2, GGCCGACCTGAGATTCCC; P3, CTCTGCATCTGTCAAGCTGG; P4, CCTTCACCAGGAAGCCCAGA.

Clones encoding PSD-93 were isolated from a rat brain cDNA library (Stratagene) by plaque hybridization.

nNOS Protein Purification and Catalytic Assays

Solubilized tissue homogenates were incubated with 100 μl of 2′5′-ADP agarose (Sigma); columns were washed with 5 ml of buffer containing 0.35 M NaCl and were eluted with 10 mM reduced nicotinamide adenine dinucleotide phosphate. Catalytic NOS activity was quantitated by monitoring the conversion of [³H]arginine to [³H]citrulline as described (Bredt and Snyder, 1990).

References

Adams, M.E., Butler, M.H., Dwyer, T.M., Peters, M.F., Murnane, A.A., and Froehner, S.C. (1993). Two forms of mouse syntrophin, a 58 kd dystrophin-associated protein, differ in primary structure and tissue distribution. Neuron 11, 531–540.

Adams, M.E., Dwyer, T.M., Dowler, L.L., White, R.A., and Froehner, S.C. (1995). Mouse α1- and β2-syntrophin gene structure, chromosome localization, and homology with a discs large domain. J. Biol. Chem. 270, 25859–25865.

Ahn, A.H., and Kunkel, L.M. (1995). Syntrophin binds to an alternatively spliced exon of dystrophin. J. Cell. Biol. 128, 363–371.

Ahn, A.H., Yoshida, M., Anderson, M.S., Feener, C.A., Selig, S., Hagiwara, Y., Ozawa, E., and Kunkel, L.M. (1994). Cloning of human basic A1, a distinct 59-kDa dystrophin-associated protein encoded on chromosome 8q23–24. Proc. Natl. Acad. Sci. USA 91, 4446–4450.

Aoki, C., Fenstemaker, S., Lubin, M., and Go, C.G. (1993). Nitric oxide synthase in the visual cortex of monocular monkeys as revealed by

light and electron microscopic immunocytochemistry. Brain Res. *620*, 97–113.

Bredt, D.S., and Snyder, S.H. (1990). Isolation of nitric oxide synthetase, a calmodulin-requiring enzyme. Proc. Natl. Acad. Sci. USA *87*, 682–685.

Bredt, D.S., and Snyder, S.H. (1994a). Nitric oxide: a physiologic messenger molecule. Annu. Rev. Biochem. *63*, 175–195.

Bredt, D.S., and Snyder, S.H. (1994b). Transient nitric oxide synthase neurons in embryonic cerebral cortical plate, sensory ganglia, and olfactory epithelium. Neuron *13*, 301–313.

Bredt, D.S., Hwang, P.M., and Snyder, S.H. (1990). Localization of nitric oxide synthase indicating a neural role for nitric oxide. Nature *347*, 768–770.

Bredt, D.S., Hwang, P.M., Glatt, C.E., Lowenstein, C., Reed, R.R., and Snyder, S.H. (1991). Cloned and expressed nitric oxide synthase structurally resembles cytochrome P-450 reductase. Nature *351*, 714–718.

Brenman, J.E., Chao, D.S., Xia, H., Aldape, K., and Bredt, D.S. (1995). Nitric oxide synthase complexed with dystrophin and absent from skeletal muscle sarcolemma in Duchenne muscular dystrophy. Cell *82*, 743–752.

Butler, M.H., Douville, K., Murnane, A.A., Kramarcy, N.R., Cohen, J.B., Sealock, R., and Froehner, S.C. (1992). Association of the Mr 58,000 postsynaptic protein of electric tissue with *Torpedo* dystrophin and the Mr 87,000 postsynaptic protein. J. Biol. Chem. *267*, 6213–6218.

Cho, K.-O., Hunt, C.A., and Kennedy, M.B. (1992). The rat brain postsynaptic density fraction contains a homolog of the Drosophila discs-large tumor suppressor protein. Neuron *9*, 929–942.

Dawson, T.M., Dawson, V.L., and Snyder, S.H. (1992). A novel neuronal messenger molecule in brain: the free radical, nitric oxide [see comments]. Ann. Neurol. *32*, 297–311.

Fields, S., and Song, O. (1989). A novel genetic system to detect protein–protein interactions. Nature *340*, 245–246.

Frohman, M.A. (1993). Rapid amplification of complementary DNA ends for generation of full-length complementary DNAs: thermal RACE. Meth. Enzymol. *218*, 340–356.

Furchgott, R.F., and Zawadzki, J.V. (1980). The obligatory role of endothelial cells in the relaxation of arterial smooth muscle by acetylcholine. Nature *288*, 373–376.

Garthwaite, J. (1991). Glutamate, nitric oxide and cell–cell signalling in the nervous system. Trends Neurosci. *14*, 60–67.

Hall, A.V., Antoniou, H., Wang, Y., Cheung, A.H., Arbus, A.M., Olson, S.L., Lu, W.C., Kau, C.L., and Marsden, P.A. (1994). Structural organization of the human neuronal nitric oxide synthase gene (NOS1). J. Biol. Chem. *269*, 33082–33090.

Hecker, M., Mulsch, A., and Busse, R. (1994). Subcellular localization and characterization of neuronal nitric oxide synthase. J. Neurochem. *62*, 1524–1529.

Hibbs, J.B., Jr., Vavrin, Z., and Taintor, R.R. (1987). L-arginine is required for expression of the activated macrophage effector mechanism causing selective metabolic inhibition in target cells. J. Immunol. *138*, 550–565.

Huang, P.L., Dawson, T.M., Bredt, D.S., Snyder, S.H., and Fishman, M.C. (1993). Targeted disruption of the neuronal nitric oxide synthase gene. Cell *75*, 1273–1286.

Huang, Z., Huang, P.L., Panahian, N., Dalkara, T., Fishman, M.C., and Moskowitz, M.A. (1994). Effects of cerebral ischemia in mice deficient in neuronal nitric oxide synthase. Science *265*, 1883–1885.

Kim, E., Niethammer, M., Rothschild, A., Jan, Y.N., and Sheng, M. (1995). Clustering of Shaker-type K$^+$ channels by direct interaction with the PSD-95/SAP90 family of membrane-associated guanylate kinases. Nature, in press.

Kistner, U., Wenzel, B.M., Veh, R.W., Cases-Langhoff, C., Garner, A.M., Appeltauer, U., Voss, B., Gundelfinger, E.D., and Garner, C.C. (1993). SAP90, a rat presynaptic protein related to the product of the *Drosophila* tumor suppressor gene dlg-A. J. Biol. Chem. *268*, 4580–4583.

Kobzik, L., Reid, M.B., Bredt, D.S., and Stamler, J.S. (1994). Nitric oxide in skeletal muscle. Nature *372*, 546–548.

Kornau, H.-C., Schenker, L.T., Kennedy, M.B., and Seeburg, P.H. (1995). Domain interaction between NMDA receptor subunits and the postsynaptic density protein PSD-95. Science *269*, 1737–1740.

Moncada, S., and Higgs, A. (1993). The L-arginine–nitric oxide pathway. N. Engl. J. Med. *329*, 2002–2012.

Nathan, C., and Xie, Q.W. (1994). Regulation of biosynthesis of nitric oxide. J. Biol. Chem. *269*, 13725–13728.

Nelson, R.J., Demas, G.E., Huang, P.L., Fishman, M.C., Dawson, V.L., Dawson, T.M., and Snyder, S.H. (1995). Behavioural abnormalities in male mice lacking neuronal nitric oxide synthase. Nature *378*, 383–386.

Peters, M.F., Kramarcy, N.R., Sealock, R., and Froehner, S.C. (1994). β2-syntrophin: localization at the neuromuscular junction in skeletal muscle. Neuroreport *5*, 1577–1580.

Sassoon, D., and Rosenthal, N. (1993). Detection of messenger RNA by in situ hybridization. Meth. Enzymol. *225*, 384–404.

Sato, T., Irie, S., Kitada, S., and Reed, J.C. (1995). FAP-1: a protein tyrosine phosphatase that associates with Fas. Science *268*, 411–415.

Schmidt, H.H., Gagne, G.D., Nakane, M., Pollock, J.S., Miller, M.F., and Murad, F. (1992). Mapping of neural nitric oxide synthase in the rat suggests frequent colocalization with NADPH diaphorase but not with soluble guanylyl cyclase, and novel paraneural functions for nitrinergic signal transduction. J. Histochem. Cytochem. *40*, 1439–1456.

Schuman, E.M., and Madison, D.V. (1994). Nitric oxide and synaptic function. Annu. Rev. Neurosci. *17*, 153–183.

Xie, J., Roddy, P., Rife, T.K., Murad, F., and Young, A.P. (1995). Two closely linked but separable promoters for human neuronal nitric oxide synthase gene transcription. Proc. Natl. Acad. Sci. USA *92*, 1242–1246.

Yang, B., Ibraghimov-Beskrovnaya, O., Moomaw, C.R., Slaughter, C.A., and Campbell, K.P. (1994). Heterogeneity of the 59-kDa dystrophin-associated protein revealed by cDNA cloning and expression. J. Biol. Chem. *269*, 6040–6044.